Control of magnetic fluctuations by spin current

V. E. Demidov[1*], S. Urazhdin[2], E. R. J. Edwards[1], M. D. Stiles[3], R. D. McMichael[3], and S. O. Demokritov[1]

[1]*Institute for Applied Physics and Center for Nonlinear Science, University of Muenster, Corrensstrasse 2-4, 48149 Muenster, Germany*

[2]*Department of Physics, West Virginia University, Morgantown, WV 26506, USA*

[3]*Center for Nanoscale Science and Technology, National Institute of Standards and Technology, Gaithersburg, MD 20899, USA*

We use micro-focus Brillouin light scattering spectroscopy to study the interaction of spin current with magnetic fluctuations in a Permalloy microdisc located on top of a Pt strip carrying an electric current. We show that the fluctuations can be efficiently suppressed or enhanced by different directions of the electric current. Additionally, we find that the effect of spin current on magnetic fluctuations is strongly influenced by nonlinear magnon-magnon interactions. The observed phenomena can be used for controllable reduction of thermal noise in spintronic nanodevices.

PACS numbers: 75.30.Ds, 85.75.-d, 75.40.Gb, 75.76.+j
* Corresponding author, e-mail: demidov@uni-muenster.de

The interplay between spin transport and magnetization, a collective property of the electrons, plays a central role in spin-based electronic devices such as magnetic memory and sensors. Operation of these devices relies on the dependence of their electronic properties on the magnetic configuration due to the magnetoresistance [1], or conversely on the ability to electrically control their magnetic configuration by the current [2]. The miniaturization of these devices is beneficial for reducing their power consumption, but thermal fluctuations of the nanoscale magnets increasingly compromise their stability. The ability to suppress thermal fluctuations will enable development of smaller and more efficient spintronic devices.

The effect of current on the magnetic configuration results from the modification of the dynamical properties of nanomagnets by the spin transfer torque (STT) [3]. In particular, STT changes the effective magnetic damping [4]. Moreover, studies of magnetization reversal in nano-elements show that STT can modify their thermal activation rates, which was interpreted as evidence for the effect of STT on thermal fluctuations [5]. This effect can be measured by noise spectroscopy in magnetic tunnel junctions with large magnetoresistance [7,8]. However, such electronic measurements require a finite dc bias and are limited to magnetic configurations producing large magnetoresistive signals.

In this Letter, we report direct measurement of the effects of spin current on the magnetic fluctuations by utilizing micro-focus Brillouin light scattering (BLS) spectroscopy, which yields a signal proportional to the spectral density of fluctuations with an unprecedented sensitivity. We show that different polarizations of the spin current enhance or suppress the fluctuations. There are three major contributions to these effects: direct influence of STT, Joule heating, and nonlinear magnon-magnon interactions redistributing the energy of fluctuations within the magnon spectrum. The relative importance of these contributions depends on the polarization and the magnitude of the spin current, as well as on the fluctuation wavelength. For example, for currents suppressing long-wavelength fluctuations, the short-wavelength fluctuations are enhanced by the Joule heating. We show that the time scales for these phenomena are significantly different, which enables fast "cooling" of the magnetic system by STT in spintronic devices.

Our test devices consist of a 5 nm thick and 2 μm in diameter $Ni_{80}Fe_{20}$ =Permalloy (Py) disk fabricated on top of a 10 nm thick and 2.8 μm wide Pt microstrip [see Fig. 1(a)]. The operation of the device relies on a torque on the

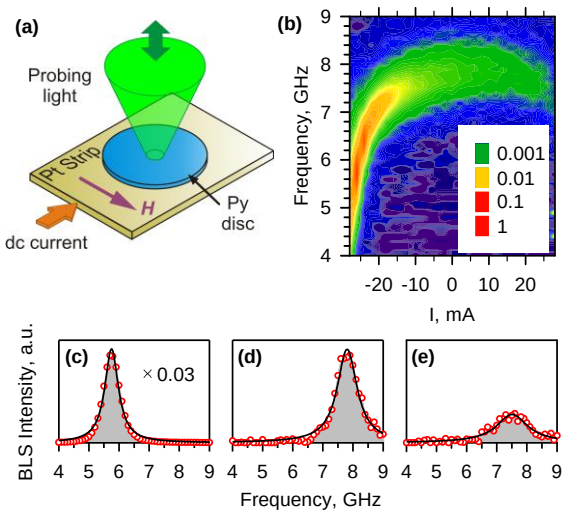

Fig. 1 (color online) (a) Schematic of the experiment. (b) Pseudocolor logarithmic map of the BLS intensity *vs* current and frequency. (c)-(e) Representative spectra acquired at I=–26, 0, and 26 mA, respectively. Curves are Lorentzian fits to the data.

magnetization in Py induced by electrical current I in the Pt strip. This torque can originate from the spin Hall effect (SHE) [9] in the bulk of the Pt producing a spin current at the interface with the Py disk [10,11]. Additional contributions to the current-induced torques can be produced by the Rashba-like effects at the interface between the Py and Pt [12], or in the Py itself [13]. We refer to any combination of these mechanisms as spin transfer torque, since each of them involves the coupling of conduction spins with the magnetization.

In contrast to the typical multilayer STT devices that require nontransparent electrical contacts to the magnetic layers, our geometry allows optical access to the surface of the Py disk. We measure the effect of STT on thermal fluctuations at room temperature by micro-focus BLS [14]. The BLS signal arises from inelastic scattering of light by spin waves, producing intensity proportional to the square of the dynamic magnetization, or equivalently to the energy associated with the magnetic fluctuations. Measurements described below probe the magnetization dynamics in a 250 nm diameter spot at the center of the Py disk, with a magnetic field $\mu_0 H$=90 mT applied in-plane perpendicular to the Pt microstrip.

Figure 1(b) shows a pseudocolor plot of the BLS intensity as a function of current and frequency. As shown in Figs. 1(c)-1(e) for I=–26, 0, and 26 mA, respectively, the BLS spectra exhibit a peak with a Lorentzian lineshape. The characteristics of the peak exhibit a strong dependence on I that is asymmetric with respect to the current direction. For I>0, for which the magnetic moments in the spin current are parallel to the magnetization, the intensity of the peak monotonically decreases with increasing I, while its central frequency remains approximately independent of I. In contrast, for I<0, for which the magnetic moments in the spin current are antiparallel to the magnetization, the intensity of the peak increases with increasing I and the central frequency exhibits a dramatic red shift at I<–26 mA. To investigate the symmetry of the effect, we performed similar measurements for different in-plane orientations of **H**. The effect of the electric current on the spectral peak is most significant when **H** is oriented perpendicular to the current, and becomes inverted with respect to the direction of current when **H** is rotated by 180°. This symmetry is expected for both the SHE [9-11] and the Rashba-like effects [12,13].

We use Lorentzian fits of the BLS spectra to determine the current dependence of the integral intensity of the spectral peak, the central frequency f_0, and the spectral full width at half maximum Δf, as shown in Figs. 2(a,b) [15]. The linear variation of Δf at small I [inset in Fig. 2(b)] is consistent with the linear effects of STT on the magnetic damping, as previously demonstrated by STT-FMR [6]. However, modification of damping alone cannot account for the dependence of the integral intensity on current [Fig. 2(a)]. The integral intensity of the BLS peak is proportional to the average fluctuation energy of the FMR mode. If the magnetic system were to behave simply as if the damping were changed while maintaining thermal equilibrium, then in the classical limit the average fluctuation energy associated with each dynamical mode would remain at a value of $k_B T$ [16]. In this case, the integral intensity would remain constant, contrary to the data of Fig. 2(a).

At I=–28 mA, the integral intensity increases by more than a factor of 30, and at I=28 mA it decreases by more than a factor of 2. These results clearly demonstrate that besides modifying the damping, STT drives the magnetic system into a nonequilibrium state. We show below that these behaviours are consistent with the established theories of STT once different contributions to the dissipation and the associated fluctuating fields are separately considered. Analysis given below

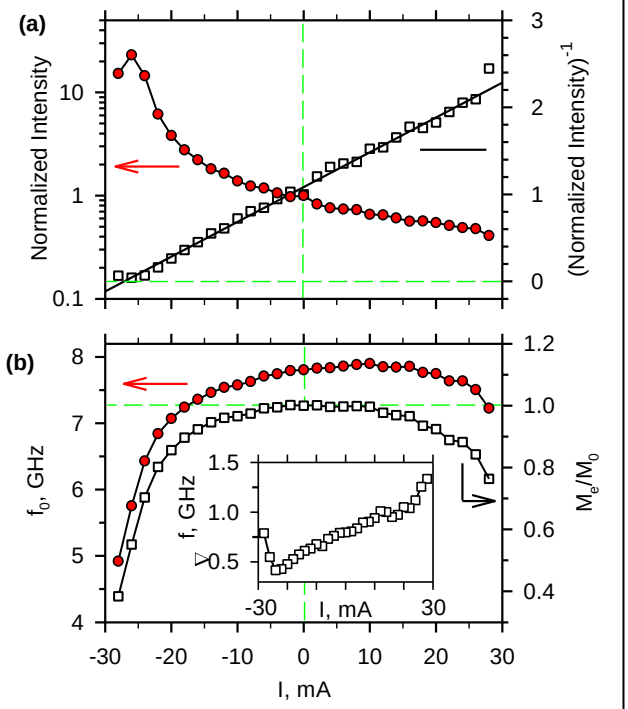

Fig. 2 (color online) (a) Normalized integral intensity under the peak (circles) and its inverse value (squares) *vs* current. Solid line is a linear fit to the data. (b) The peak central frequency (circles) and calculated effective magnetization normalized by its value at I=0 (squares) *vs* current. Inset shows the linewidth of the peak *vs* current.

predicts a linear dependence of the inverse integral intensity on current, in agreement with the data shown in Fig. 2(a) by squares.

Extrapolating the low-current linear variations of the inverse intensity, we estimate the critical current I_c =–28 mA, at which the intensity of the BLS peak can be expected to diverge. Instead, it saturates and starts to decrease at I<–26 mA [Fig. 2(a)], while the linewidth of the peak increases [inset in Fig. 2(b)]. These behaviours suggest an onset of a new relaxation process limiting the amplitude of magnetic fluctuations.

The central frequency f_0 of the peak exhibits a red shift at I<0 [circles in Fig. 2(b)], which we attribute to a decrease of the effective magnetization M_e due to the increased intensity of magnetic fluctuations. We determine M_e from our measurements of f_0 using the Kittel formula $f_0^2 = \gamma^2\mu_0^2 H(H+M_e)$ [17], where γ is the gyromagnetic ratio and H is the magnetic field corrected by the Oersted field, the correction being 6 mT at the maximum current of 28 mA. The resulting dependence of M_e on I exhibits a monotonic

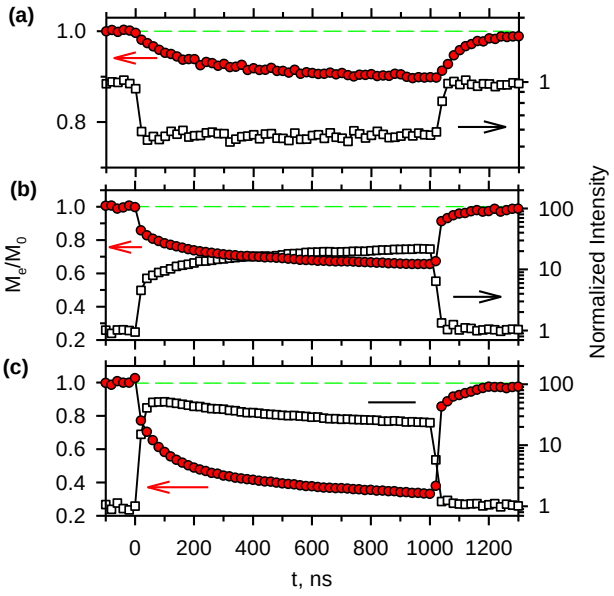

Fig. 3 (color online) Temporal evolution of the normalized effective magnetization (circles) and the normalized integral BLS peak intensity (squares) resulting from a 1 μs-long pulse of current I applied at t=0: (a) I=25 mA, (b) I=–25 mA, (c) I=–30 mA.

decrease at I < -26 mA [Fig. 2(b)].

We attribute the different behaviors of M_e and of the intensity to different effects of STT on the amplitudes of different spin wave modes. BLS spectra are selectively sensitive to the fluctuations with a long wavelength, while f_0 (or M_e) characterizes the total fluctuation intensity of the entire spin-wave ensemble, dominated by the large phase volume of short-wavelength spin waves. The BLS intensity saturates [Fig 2(a)], while the effective magnetization decreases monotonically [Fig. 2(b)]. Therefore, we conclude that as the current approaches the critical value, short-wavelength fluctuations are continuously enhanced, while the intensity of long-wavelength fluctuations saturates. This disproportional enhancement of different spin wave modes indicates that magnetic system driven by STT is strongly out-of-equilibrium.

To elucidate the mechanisms contributing to the observed phenomena at large currents and to separate the effects of STT from the Joule heating, we performed time-resolved BLS measurements of fluctuations in the presence of 1μs long current pulses with a 5 μs repetition period. Figure 3 shows the temporal evolution of the integral BLS peak intensity (squares) and of the effective magnetization M_e (circles) for three values of I.

At I=25 mA [Fig. 3(a)], where suppression of fluctuations is observed in the static

measurements, the BLS intensity rapidly decreases by a factor of two at the onset of the pulse, remains constant over the pulse duration, and rapidly rises again to the original value at the end of the pulse. The timescale for these intensity variations is shorter than the 20 ns resolution limit of our measurement. In contrast, M_e exhibits a gradual exponential decrease at the beginning of the pulse followed by a similar slow relaxation after its end, characterized by a time constant $\tau \approx$ 90 ns.

The timescale for the effects of STT is determined by the magnetic relaxation rate which is typically a few nanoseconds. On the other hand, the timescale for the Joule heating is determined by a much slower rate of heat diffusion away from the device. Therefore, one can conclude that in the fluctuation-suppression regime, the long-wavelength part of the fluctuation spectrum is rapidly and efficiently cooled by STT, while the total intensity of fluctuations dominated by the short-wavelength modes is slowly enhanced due to the Joule heating.

In the fluctuation-enhancement regime at $I<0$, the temporal evolution of fluctuations is qualitatively different [Figs. 3(b,c)]. Both the intensity and M_e rapidly change at the onset of the pulse, and subsequently vary with a much longer characteristic timescale. At the end of the pulse, M_e first rapidly increases, and then slowly relaxes with a time constant $\tau \approx 90$ ns. These results enable us to separate the contribution of STT from the Joule heating. The rapid increase of M_e at the end of the pulse can be attributed to the relaxation of the magnetic system into equilibrium with the lattice. This process is characterized by the spin-lattice relaxation rate of a few nanoseconds. The subsequent slow relaxation of M_e is associated with the simultaneous cooling of the lattice and the magnetic system. Therefore, by comparing the magnitudes of the fast and the slow variations of M_e at the end of the pulse, we conclude that the contribution of the Joule heating to the total enhancement of fluctuations does not exceed 30 %. Moreover, the contribution of the slow relaxation to the BLS intensity is negligible, demonstrating that the Joule heating mainly affects short-wavelength fluctuations.

The temporal evolution of M_e is similar for I=-25 mA and I=-30 mA, as illustrated in Figs. 3(b) and (c), respectively. Surprisingly, the evolution of the BLS intensity at the onset of the pulse is qualitatively different for these two values of I. At I=-25 mA, the intensity rapidly increases at the onset of the pulse, and subsequently continues to slowly rise. In contrast, at I=-30 mA the intensity initially rapidly increases, but then slowly *decreases* over the rest of the pulse duration.

We attribute the origin of these different temporal behaviours to the same nonlinear dynamical mechanisms that lead to the saturation of intensity in the static measurements at $I<-26$ mA [Fig. 2(a)]. Since the initial increase of intensity at I=–30 mA is significantly larger than at I=–25 mA, it is the subsequent slow variation that results in the saturation in Fig. 2(b). By examining the temporal evolution of both M_e and the intensity, we conclude that the fluctuations of both the long- and the short-wavelength modes are initially significantly more enhanced at I=–30 mA than at I=–25 mA, resulting in stronger nonlinear magnon-magnon scattering that redistributes the energy within the fluctuation spectrum. While the details of these nonlinear scattering processes are yet unknown, they can be generally expected to drive the magnetic subsystem towards a thermal distribution [18], thus suppressing the intensity of the FMR-mode fluctuations close to the critical current and preventing the onset of auto-oscillation.

To analyze the observed effects of STT on the magnetic fluctuations, we use the Landau-Lifshitz-Gilbert-Slonczewski equation

$$\dot{\mathbf{M}} = -\gamma \mathbf{M} \times \mu_0 \mathbf{H}_{\text{eff}} + \frac{\alpha}{M_s} \mathbf{M} \times \dot{\mathbf{M}} + \frac{\beta}{M_s^2} \mathbf{M} \times (\mathbf{M} \times \hat{\mathbf{y}}) \quad , \quad (1)$$

where α is the damping parameter, β is the strength of the spin transfer torque, which is proportional to the electric current, and M_s is the saturation magnetization. The effective field H_{eff} is a sum of the external field $\mathbf{H}_0$ directed along the y-axis, the dipolar field, and a fluctuating field H_T determined by the fluctuation-dissipation relation. Solving this equation in the linearized limit $\mathbf{M} = M_s\ (m_x, 1, m_z)$, where m_x, $m_z << 1$, and assuming that the thermal fluctuation field is independent of the current, we find the average energy in each spin-wave mode

$$\langle E_i \rangle = k_B T \frac{\Gamma_i}{\Gamma_i - \beta}. \quad (2)$$

Here, Γ_i characterizes the damping and line width of mode i, $\Gamma_0 = \alpha\gamma\mu_0(H + 0.5M_s)$ for the FMR mode, and $\Gamma_i = \alpha\gamma\mu_0(H + 0.5M_s + Dk_i^2 + G(\mathbf{k}_i))$ for a mode with a wave vector $\mathbf{k}_i$, where D is the exchange constant and $G(\mathbf{k}_i)$ gives wave vector-

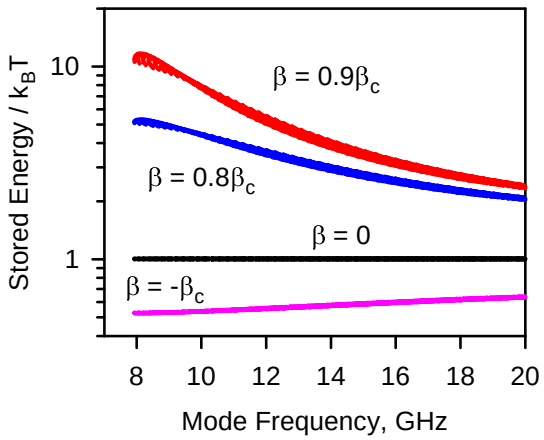

Fig. 4 (color online) Calculated average fluctuation energy per mode at the labeled values of the strength of the spin transfer torque β normalized by its critical value β_c. The spread in energy at a given frequency and β is caused by the variations of the damping rates Γ_i among different modes with the same frequency.

dependent dipolar corrections [19]. Equation (2) shows that STT modifies the fluctuation intensity, such that the inverse of the average energy in each mode scales linearly with β (or the current), in agreement with the data of Fig. 2(a).

Equation (2) allows us to calculate the effects of STT on the spin wave distribution, as shown in Fig. 4 for several values of β scaled by the critical value $\beta_c = \Gamma_0$, corresponding to the critical current I_c. The calculation for $\beta = -\beta_c$ in Fig. 4 yields a distribution with the average energy of low-frequency (long-wavelength) modes reduced by a factor of 2, in agreement with our experimental data for $I = -I_c = 28$ mA [Fig. 2(a)]. In contrast, for β approaching β_c, the average energy of the low-frequency modes diverges. This result differs from our experimental observation of average energy saturation, since the calculation does not take into account the nonlinear spin wave scattering processes that saturate the intensity of the FMR mode. Nevertheless, the calculations of Fig. 4 show that STT disproportionately enhances the intensity of the low-frequency modes, resulting in a strongly nonequilibrium spin wave distribution, and consequently in significant nonlinear scattering effects.

In summary, we have directly measured the effects of spin current on thermal fluctuations in microscopic magnetic elements. We show that spin current interacts with all spin-wave modes, and causes strong nonlinear interactions at driving currents close to the critical value. Our results provide insight into the complexity of STT-induced phenomena and suggest a route for controllable manipulation of fluctuations in magnetic nanodevices.

We acknowledge support from Deutsche Forschungsgemeinschaft, the European Project Master (No. NMP-FP7 212257), the NSF grants DMR-0747609 and ECCS-0967195, and the Research Corporation.

REFERENCES

[1] M.N. Baibich *et al.*, Phys. Rev. Lett. **61,** 2472 (1988); G. Binasch *et al.*, Phys. Rev. B **39,** 4828 (1989).
[2] D. C. Ralph and M. D. Stiles, J. Magn. Magn. Mater. **320**, 1190 (2008).
[3] J.C. Slonczewski, J. Magn. Magn. Mater. **159**, L1 (1996); L. Berger, Phys. Rev. B **54**, 9353 (1996).
[4] I.N. Krivorotov *et al.*, Science **307**, 228 (2005).
[5] S. Urazhdin *et al.*, Phys. Rev. Lett. **91**, 146803 (2003); I.N. Krivorotov *et al.*, Phys. Rev. Lett. **93**, 166603 (2004).
[6] J. C. Sankey *et al.*, Phys. Rev. Lett. **96**, 227601 (2006).
[7] A. M. Deac *et al*. Nature Phys. **4**, 803 (2008).
[8] A. Helmer *et al.*, Phys. Rev. B **81**, 094416 (2010).
[9] M. I. Dyakonov and V. I. Perel, Sov. Phys. JETP Lett. **13,** 467 (1971); J.E. Hirsch, Phys. Rev. Lett. **83**, 1834 (1999).
[10] K. Ando *et al.*, Phys. Rev. Lett. **101**, 036601 (2008); L. Liu *et al.*, Phys. Rev. Lett. **106**, 036601 (2011).
[11] O. Mosendz *et al.*, Phys. Rev. Lett. **104**, 046601 (2010).
[12] I. M. Miron *et al.*, Nature Mater. **9**, 230 (2010).
[13] A. Manchon and S. Zhang, Phys. Rev. B **79**, 094422 (2009); A. Chernyshov *et al.*, Nature Phys. **5**, 656 (2009).
[14] S. O. Demokritov and V. E. Demidov, IEEE Trans. Mag. **44**, 6 (2008).

[15] Lorentzian fits to the BLS sprectra give mean uncertainties for f_0, Δf, and J of <1 %, 3 %, 2 %, respectively; the corresponding error bars are smaller than the symbol sizes used in the plots.
[16] J. Weber, Phys. Rev. **101**, 1620 (1956).
[17] C. Kittel Phys. Rev. **73**, 155 (1948).
[18] S. M. Rezende at al., Phys. Rev. B, **73**, 094402 (2006); V. E. Demidov et al., Phys. Rev. Lett. **99**, 037205 (2007).
[19] B.A. Kalinikos and A.N. Slavin, J. Phys. C **19**, 7013 (1986).